D. What the Solutions Mean

We now have all the theory we need to interpret glacial rebound and infer the viscosity of the earth's mantle, but the meaning of these solutions are not yet clear. To make them clear we will first examine the solutions we have obtained in some detail. We will then develop a simple method for examining glacial rebounds of various scales to infer the viscosity profile of the earth. Finally we will return to some critical details and present some computer solutions. The sequence of extensive theory → insights + simplifications → back of the envelope analysis of physical processes → modeling + testing of subtler insights is a common cycle in my experience.

1. Flow in a uniform viscosity half-space

Equation (22) describes the flow produced by a 1 Nm^{-2} harmonic load applied to the surface of a fluid half space. To visualize more physically, consider the harmonic load $\bar{\tau}_{zz}$ to be a small deformation of the surface of amplitude h:

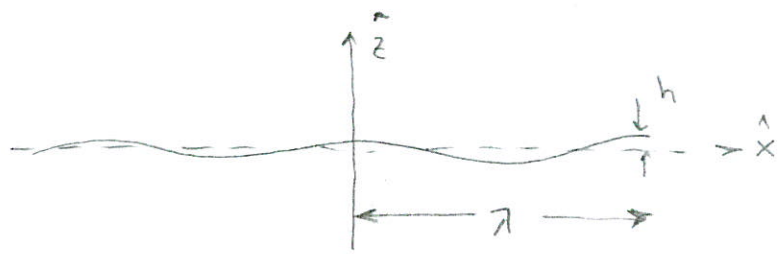

The vertical stress is then $\tau_{zz} = -\rho g h \cos kx$, where $k = 2\pi/\lambda$. The fourier transform $\bar{\tau}_{zz} = -\rho g h$, and equation (22) becomes:

$$\begin{bmatrix} 2\eta^* i k \bar{v}_z \\ 2\eta^* k \bar{v}_z \\ i\bar{\tau}_{xz} \\ \bar{\tau}_{zz} \end{bmatrix} = \rho g h e^{kz} \left[\begin{pmatrix} 0 \\ -1 \\ 0 \\ -1 \end{pmatrix} + kz \begin{pmatrix} -1 \\ 1 \\ -1 \\ 1 \end{pmatrix} \right] \qquad (22a)$$

The flow response is the real part of the Fourier transform (c):

$$f(x) = \int_{-\infty}^{\infty} F(k)\, e^{ikx}\, dk.$$

Since $e^{ikx} = \cos kx + i \sin kx$, for a single value of k:

(22b)

$$v_x = -\frac{\rho g h}{2\eta^* k}\, kz\, e^{kz} \sin kx$$

$$v_z = \frac{\rho g h}{2\eta^* k} (kz - 1)\, e^{kz} \cos kx .$$

The horizontal and vertical velocities decrease nearly exponentially with depth. v_x is zero at the surface and at $x = 0, \lambda/2 \ldots$ but increases to a maximum at $z = \lambda/2\pi$ at $x = \lambda/4, 3\lambda/4 \ldots$ At the surface v_z is a maximum at $x = 0, \pi, 2\pi, \ldots$

The response under a load (eg. $x=0$) is

$v_z(x=0, t=0) = -\dfrac{\rho g h}{2\eta^* k}$. Flow lines can be sketched:

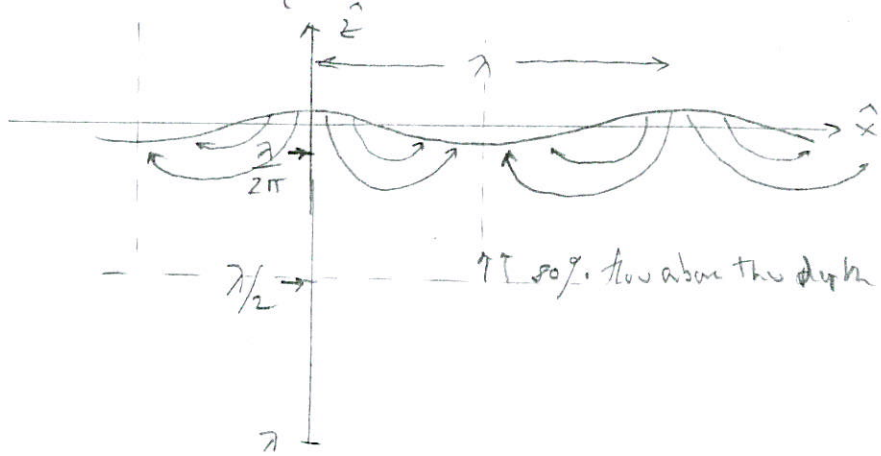

The flow described by (22a,b) is an instantaneous flow rate. At $x=0$, $z=0$, $t=0$ $v_z(x=0, z=0, t=0) = \frac{-\rho g h}{2\eta^+ k}$

Since $v_z = \frac{\partial h}{\partial t}$ it is clear the amplitude of the initial harmonic deformation of the fluid surface will decay exponentially:

(26) Deep flow

$$\boxed{h = h_0 e^{-t/\tau}, \quad \tau = \frac{2\eta^+ k}{\rho g}}$$

Since $k = 2\pi/\lambda$, it is clear from (26) that longer wavelength surface deformations will have proportionally shorter decay times (τ). Since high frequencies of a square edged initial surface deformation are composed of short wavelengths (high frequencies), uplift of an area loaded by a glacier that has melted will look something like:

DEEP FLOW

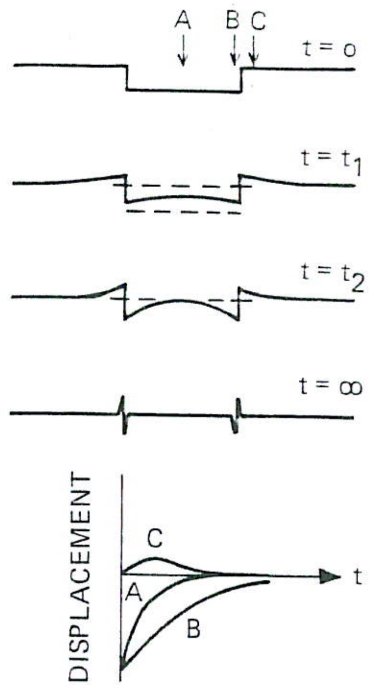

The depth to which significant flow persists can be easily estimated. From 22b

$$\frac{v_z}{v_z(z=0)} = -(zk-1)e^{kz}$$

which can be evaluated:

zk	$\frac{v_z}{v_z(z=0)}$
0	1
−1	.736
−2	.406
−3	.199

← 50% @ $zk = -1.66$

← 80% @ $zk = -3$

Fifty percent of the flow beneath a load of wavenumber $\frac{2\pi}{k}$ occurs above a depth of $zk = -1.66$; 80% above a depth of $zk = -3$. For $zk = -3$,

$$z = \frac{-3\lambda}{2\pi} \cong \tfrac{1}{2}\lambda .$$

Eighty percent of the flow occurs above a depth of $\frac{1}{2}\lambda$.

2. Flow in a Viscous Channel

For a viscous channel that is thin compared to λ, we saw from (23) that the vertical flow becomes

$$\bar{v}_z = \frac{\rho g h}{2\eta^* k}\left(\frac{2}{3}(kD)^3\right) = \frac{\rho g k^2 D^3}{2\eta} h$$

Thus

(27) Channel flow

$$\boxed{h = h_0 e^{-t/\tau_c}, \quad \tau_c = \frac{2\eta}{\rho g k^2 D^3}}$$

The short wavelengths decay much faster because here $\tau \propto \lambda^2$, and in fact heat conduction a very good analogue for the uplift response. For heat conduction short wavelengths also decay in proportion to their wavelength squared. For example the heat conduction equation

$$\frac{\partial T}{\partial t} = \kappa \nabla^2 T$$

can be solved for $T = T(t) \cos kx$

$$\frac{\partial T}{\partial t} = -k^2 \kappa T$$

(28) $$\boxed{T = T_0 e^{-t/\tau_{HC}}, \quad \tau_{HC} = \kappa k^2}$$

Thus a square edged depression will uplift like it was a cool rod being heated by its surroundings. The edges of the depressed zone will

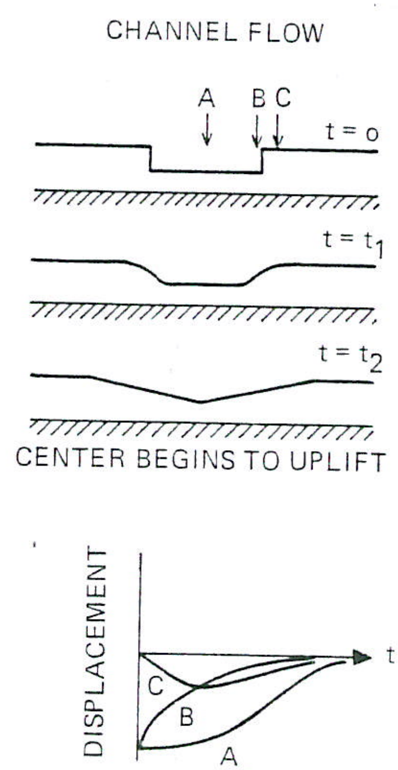

uplift first, cooling (depressing) the immediate surroundings (C).

with time the surroundings will start to warm again (uplift), and the centre will start to slowly heat (uplift) Notice, by comparison to the figure on page 31 that the uplift of regions near a deglaciated area will be opposite for deep (uplift followed by depression) and channel (depression followed by uplift) flow, and the uplift of the central regions will be fastest for deep flow whilst the uplift of near-edge areas will be fastest for channel flow. Clearly the uplift in the central parts of a glaciated area and the uplift of peripheral areas will tell us a great deal about the viscosity structure of the mantle.

3. The Lithosphere

What about the lithosphere? It acts like a low pass filter. Short wavelengths are supported elastically and will display no viscous response. Long wavelengths will not be supported by the lithosphere at all. Intermediate wavelengths will be partly supported elastically and cause some mantle flow to become, after some de partly supported by the fluid mantle. Their adjustment will be driven (unloading) or retarded (loading) by elastic as well as gravitational forces.

From (25a) the equilibrium stress at the surface equals $\rho g \alpha$ times whatever the displacement is at the base. By equilibrium stress we mean the stress <u>supported</u> by the elastic bending of the lithosphere plus the buoyant forces arising from $\bar{u}_z^B$, the deformation at the base of the lithosphere. The flow rate at the base of the lithosphere $\bar{v}_z^B$ is driven by the difference between the stress applied to the surface, ${}^{app}\tau^T_{zz}$,

and the supported stress ${}^{supt}\tau^T_{zz} = \rho g \alpha u^B_z$. As in (22)

$$v^B_z = \frac{\partial u^B_z}{\partial t} = -\left\{ \frac{{}^{app}\tau^T_{zz} - {}^{supt}\tau^T_{zz}}{2\eta^* k} \right\}$$

$$= -\left\{ \frac{{}^{app}\tau^T_{zz} - \rho g \alpha u^B_z}{2\eta^* k} \right\}$$

$$\int_{u^B_{z0}}^{u^B_z} \frac{\partial u^B_z}{{}^{app}\tau^T_{zz} - \rho g \alpha u^B_z} = -\int_0^t \frac{dt}{2\eta^* k}$$

(29) $$\boxed{\frac{\rho g \alpha u^B_z - {}^{app}\tau^T_{zz}}{\rho g \alpha u^B_{z0} - {}^{app}\tau^T_{zz}} = e^{-\rho g \alpha t / 2\eta^* k}}$$

If $u^B_{z0} = 0$

$$u^B_z(t) = \frac{{}^{app}\tau^T_{zz}}{\rho g \alpha}\left(1 - e^{-\alpha t/\tau}\right)$$

Thus the ultimate load depression is filtered by $\frac{1}{\alpha}$ and the decay time reduced by $1/\alpha$. Note $\tau = \frac{2\eta^* k}{\rho g}$

If ${}^{app}\tau^T_{zz} = 0$, $u^B_z = u^B_{z0}\, e^{-\alpha t/\tau}$ and adjustment

The deformation at the base of the lithosphere is accelerated by α

E. A First-Pass at the Mantle Viscosity Profile

We now know how a harmonic load redistribution flow in asthenosphere and mantle. We can calculate how a suddenly applied load will exponentially approach isostatic equilibrium, and how deep into the asthenosphere or mantle flow will be induced. How can we most easily infer the viscosity profile of the mantle from observed rebound data? Perhaps the easiest way is to look at the response at the centers of loads of various sizes, and characterize the central response with an equivalent wave number, k_{ctr}. The center of a load is characterized by the longest wavelength harmonic components, so it is reasonable to suppose such a characterization would work. We first find k_{ctr} in terms of load dimensions by looking at the central uplift of a cylindrical and a bar load.

we then deduce the viscosity profile of the mantle by looking at isostatic response of loads varying from ~60 km (minor ice retreat in Greenland and drainage of Lake Bonneville) to large load (1000 km ice sheet in Fennoscandia, 3000 km ice sheet in Canada) and finally very large loads (increase in meltwater to oceans).

1. A wave number to Characterize Isostatic response in the center of a load

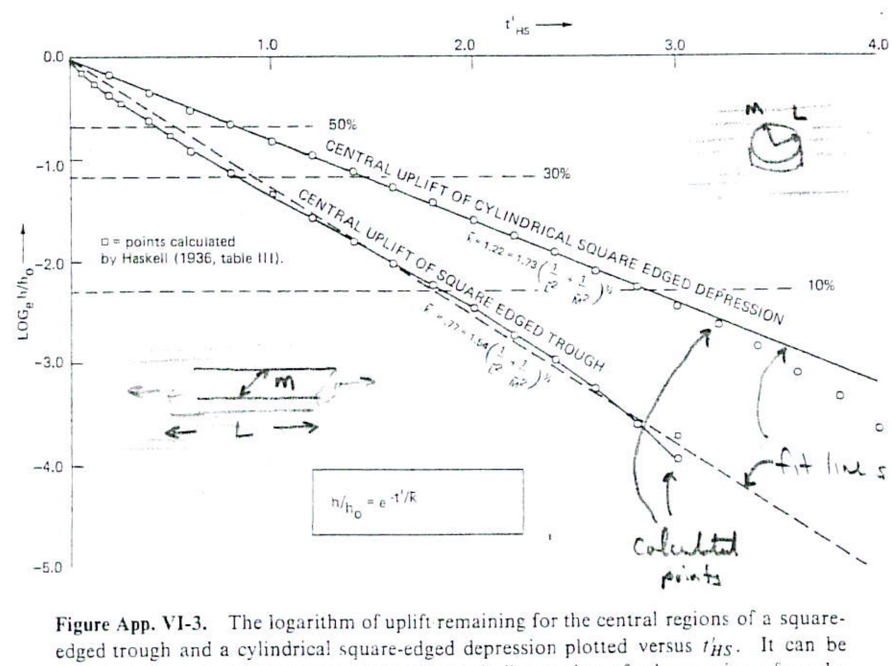

Figure App. VI-3. The logarithm of uplift remaining for the central regions of a square-edged trough and a cylindrical square-edged depression plotted versus t'_{HS}. It can be seen that the central uplift is exponential and similar to that of a harmonic surface deformation with wave number $\bar{\bar{k}} = 1.7\left(\frac{1}{\tilde{L}^2} + \frac{1}{\tilde{M}^2}\right)$. $\tilde{L}$ and $\tilde{M}$ are characteristic dimensions of the initial deformation in normalized units (see equation 5). The values calculated numerically for the square-edged trough are compared to the values calculated analytically and given by Haskell. A uniform viscosity half-space is assumed.

So to good approximation:

$$k_{ctr} = 1.7\left(\frac{1}{L^2} + \frac{1}{m^2}\right)^{1/2}$$

$\left(\lambda_{ctr} = 2.6\,D\right)$

$$= 1.7\left(\frac{1}{(2R)^2} + \frac{1}{(2R^2)}\right)^{1/2} = \frac{1.2}{R}$$

$\left(\lambda_{ctr} = 3.7\,W\right)$

$$=_{w} 1.7\left(\frac{1}{\infty^2} + \frac{1}{W^2}\right) = \frac{1.7}{W}$$

80% of the flow occurs above $z k_{ctr} = 3$. Thus

$$z_{80\%} = 2.5\,R$$

$$= 1.7\,W$$

2. Isostatic Rebound Data

Selected rebound data is shown in the following figures. We will proceed from small scale glacial unloading to large.

a. Smallest Scale

The first figure shows uplift of the land surface at various sites in Canada. Two classes of curves are apparent: one with strong curvature (M, F, G, and D) and another set of weaker curvature. The first set is associated with the last stages of deglaciation. The Greenland curve is particularly interesting as the uplift there is associated with a relatively minor (60 km) retreat of the ice cap still present on Greenland.

$$k_{cr}^{\text{Greenland}} = \frac{1.7}{60} = 0.028\ \text{km}^{-1}$$

$\tau \cong$ time to reach 2/3 isostatic equilibrium $\cong$ 1000 yrs

$\alpha \cong 2$ (assuming flexural rigidity similar to Dawson + Range)

$$\tau = \frac{2\eta k}{\alpha \rho g}, \quad \eta = \frac{\alpha \rho g \tau}{2k} = \frac{(2)(3170)(10)(1000 \cdot 3.15}{(2)(0.028 \times 10^{-3}\ \text{m}^{-1})}$$

$$\boxed{\eta = 3.5 \times 10^{19}\ \text{Pa}\cdot\text{s}}$$

$$k z_{80\%} = 3, \quad z_{80\%} = \frac{3 \cdot 60}{1.7} = 100\ \text{km}$$

$$\boxed{z_{80\%} = 100\ \text{km}}$$

The Greenland uplift suggests a very fluid asthenosphere that is at least ~ 100 km thick

The second figure shows the size and geometry of pleistocene Lake Bonneville. Shorelines in the central area are uplifted 65 m relative to the same shorelines at the edge of the lake.

$$\text{Maximum uplift} = \frac{(305\,m)(1\,g/cc\ \text{water})}{(3.17\,g/cc)} = 96\,m$$

$\tau \lesssim 4000$ yrs to achieve 65 m differential uplift

$$k_{cr} \cong \frac{1.2}{95\,km} = 1.26 \times 10^{-2}\ km^{-1}$$

$\alpha < 1.42$ (highest possible for 65 m displacement under 305 m load)

$= 1.03$ (for Walcott's flexural rigidity of 0.5×10^{23} N-m for Bonneville max)

$$\eta = \frac{\alpha \rho g \tau}{2k} = \frac{(1 \text{ to } 1.4)(3170)(10)(4000 \times 3.15 \times 10^{7})}{(2)(1.26 \times 10^{-5}\ m^{-1})}$$

$= 1.6$ to 2.2×10^{20} Pa.s

$$Z_{80\%} = \frac{3R}{1.2} = 237 \text{ km}$$

$$U_z^{elastic} = \frac{\rho_w g h}{2\mu k} = \frac{(1000)(10)(305)}{(2)(0.7\times10^{11}\text{ Pa})(1.26\times10^{-5}\text{ m}^{-1}}$$

$$U_z^{elastic} = 1.72 \text{ m}$$

6. Intermediate Scale – Fennoscandia

The third set of figures show the Fennoscandian glacier loss ~ 550 km in radius and uplifted at an exponentially decreasing rate near its center (Angerman River), with $\tau = 4400$ yrs. For such a large load $\alpha = 1$

$$k = \frac{1.2}{550 \text{ km}} = 2.18\times10^{-3} \text{ km}^{-1}$$

$$\eta = \frac{\alpha \rho g \tau}{2k} = \frac{(1)(3170)(10)(4400\times3.15\times10^7)}{(2)(2.18\times10^{-6}\text{ m}^{-1})}$$

$$= 1\times10^{21} \text{ Pa}\cdot\text{s}$$

$$Z_{50\%} = \frac{(3)(550)}{1.2} = 1375 \text{ km}$$

c. Large scale loads

The 4th set of figures show the uplift in North America. $R = 1650$, $\tau \sim 2500$ yrs. Thus

$$\frac{\eta_{canada}}{\eta_{fennosc}} = \frac{\tau_{canada}}{\tau_{fennosc}} \frac{R_{canada}}{R_{fennosc}}$$

$$\eta_{canada} = 10^{21} \text{ Pa.s} \left(\frac{2500}{4400}\right)\left(\frac{1650}{550}\right)$$

$$= 1.7 \times 10^{21} \text{ Pa.s}$$

$$z_{80\%} = \frac{3 \cdot 1650}{1.2} = 4123 \text{ km} = \text{whole mantle}$$

The ocean basins ($R \sim 3000$ km) must respond with $\tau \lesssim 2000$ yrs to avoid holocene high sea levels on the continental margins (which are not observed).

$$\eta_{ocean\ basin} = 10^{21} \text{ Pa.s} \left(\frac{2000}{4400}\right)\left(\frac{3000}{550}\right) = 2.5 \times 10^{21} \text{ Pa.s}$$

$$z_{80\%} = \frac{3 \cdot 3000}{1.2} = \text{whole mantle!}$$

The P_2 bulge must relax with $\tau < 1500$ yrs to be compatible with eclipse data.

3. Summary

Location	τ [yrs]	Scale [km]	η [Pa·s]	$z_{80\%}$ [km]	α
Greenland	1000	L = 60	3.5×10^{19}	100	2
Bonneville	4000	R = 95	1.6 to 2.2×10^{20}	237	1.42±.1
Fennoscandia	4400	R = 550	10^{21}	1375	1
Canada	2500	R = 1650	1.7×10^{21}	4123	1
Ocean Basins	< 2000	R = 3000	2.5×10^{21}	7500	1

See plot of this data
(Cont figure)

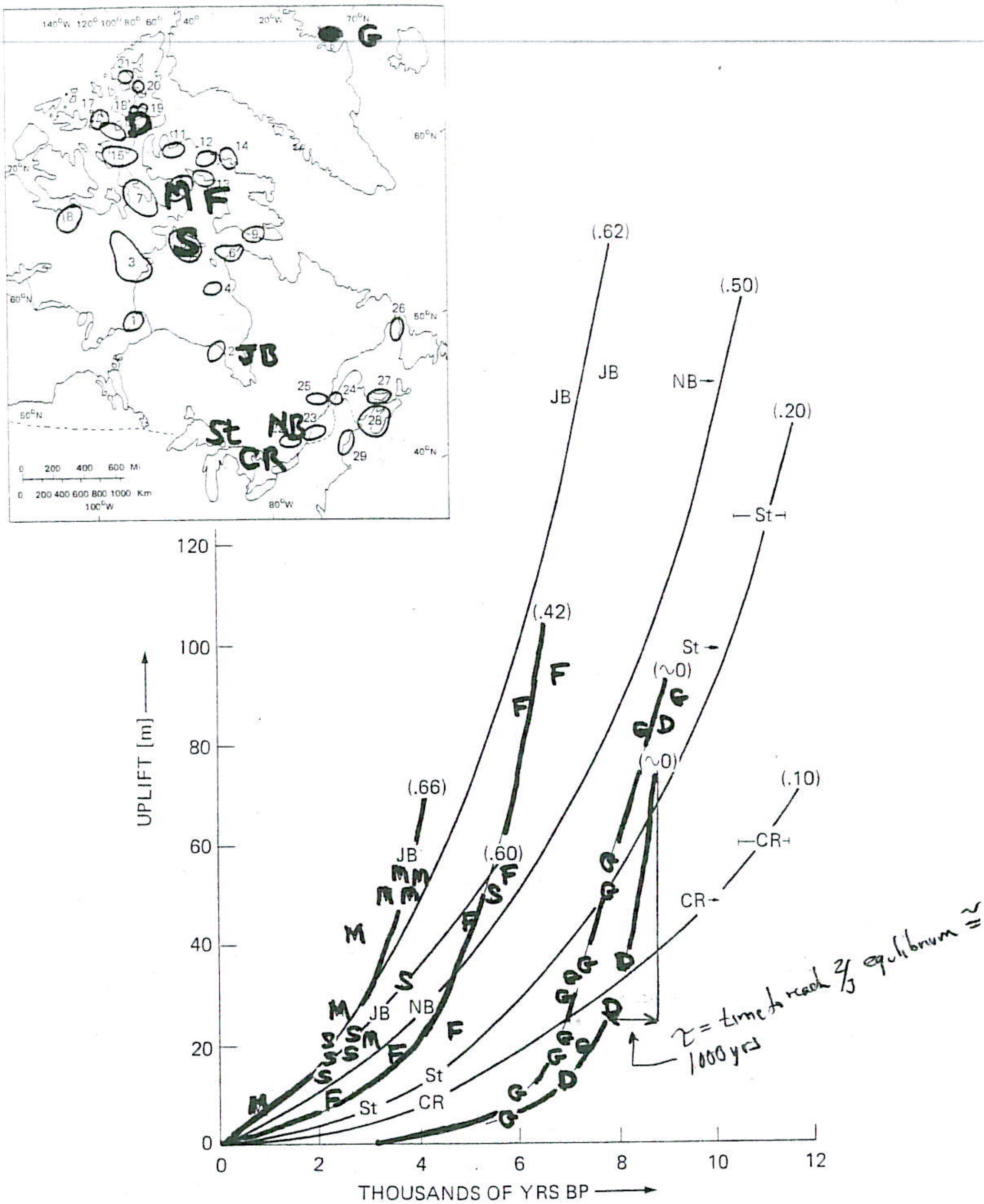

Figure IV-23. Isostatic uplift curves of Arctic Canada. The emergence curves compiled by various workers have been converted to uplift curves using Morner's eustatic sea level curve. Locations are identified in Figure App. VII-6. M = E. Melville Penin. (Farrand, 1962); JB = James Bay (Farrand, 1962); S = Southampton (Farrand, 1962); NB = North Bay (Farrand, 1962); F = N. Fox Basin (West Baffin Island); (Andrews, 1966; Ives, 1964); St = Sault (Farrand, 1962); CR = Cape Rich (Farrand, 1962); G = Greenland (Laska, 1966) D = Devon Island (Müller and Barr, 1966). The present rate of uplift estimated from the initial part of each curve is given in m/100 yrs in parentheses at the top of each curve.

Example of Lake Bonneville

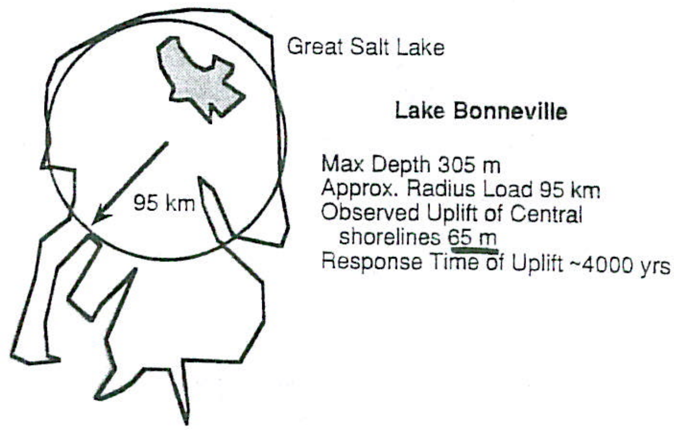

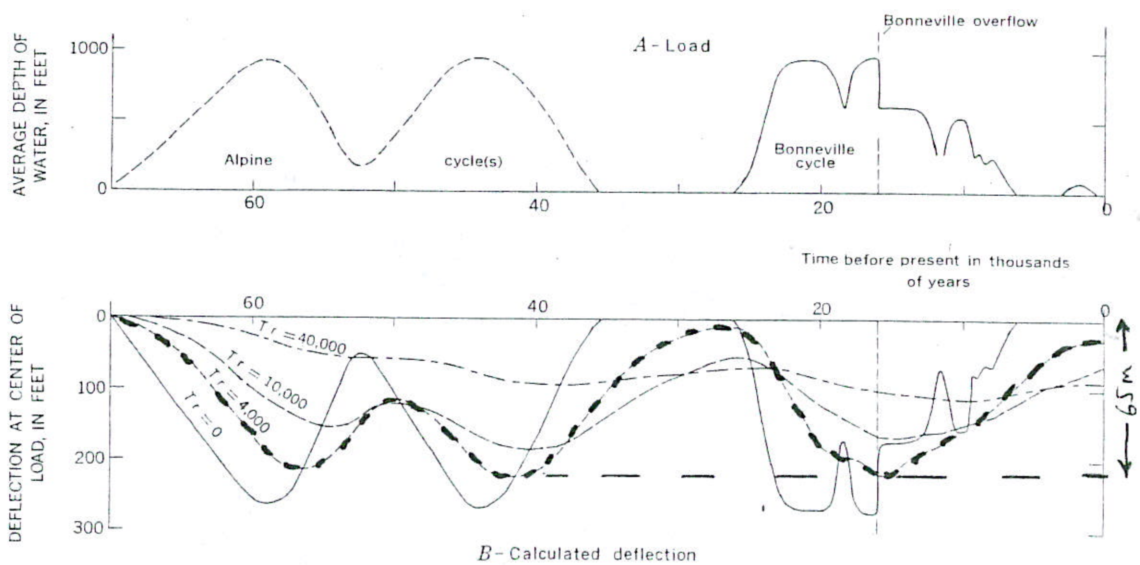

Figure IV-22. The isostatic response of Lake Bonneville. The top chart shows the loading history of Lake Bonneville. The bottom figure shows that, unless central Bonneville can be characterized by a viscous decay constant of 4,000 years or less, it could not have tracked the loading history closely enough to register a 65 m uplift today. The figures, reproduced with the author's permission, are from M. D. Crittenden, *Journal of Geophysical Research*, *68*, p. 5525, © 1963 the American Geophysical Union.

Crittenden, 1961

Figure IV-8. Isochron map showing, schematically in 1000 year lines, the retreat of the ice in Fennoscandia. The figure, reproduced with the publisher's permission, is from G. De Geer, *Geologiska Föreningens I. Stockholm Förhandlingar*, 76, p. 304, 1954, Geologiska Föreningen. *Note:* figure also appears in Woldstedt (1958).

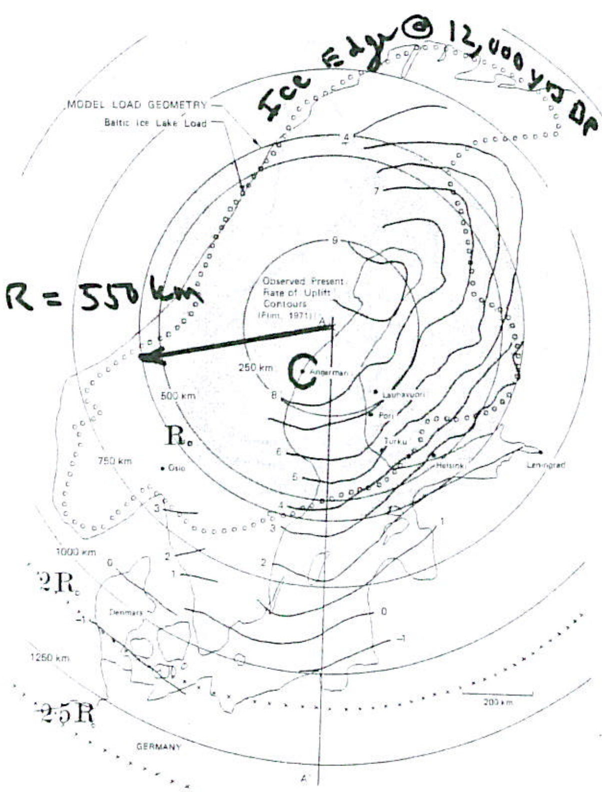

Years before 2000 AD	Emergence curve (elevation of shore-lines above present sea level)	Land uplift relative to present (Emergence curve corrected by Morner's sea level curve)	Meters from isostatic equilibrium (uplift curve plus 30 m)
9200	280	310	340
9042	219	244	274
8839	194	212	242
7944	138.9	157.9	187.9
6741	104.1	113.1	143.1
6178	90.4	95.6	125.6
5713	80.2	84.0	114.0
5535	76.2	79.7	109.7
4354	54.4	55.9	85.9
4094	51.1	52.1	82.1
3918	48.2	48.2	78.2
3408	40.7	40.7	70.7
2365	26.3	26.3	56.3
1779	18.0	18.0	48.0
1317	12.2	12.2	42.2
939	8	8	38
539	2	2	32
87	0	0	30

Table IV-10 Uplift at mouth of Angerman River, Sweden. Data are taken from Lliboutry (1972, Table 1), but are originally from Liden (1938). The last column is plotted versus first in Figure IV-38.

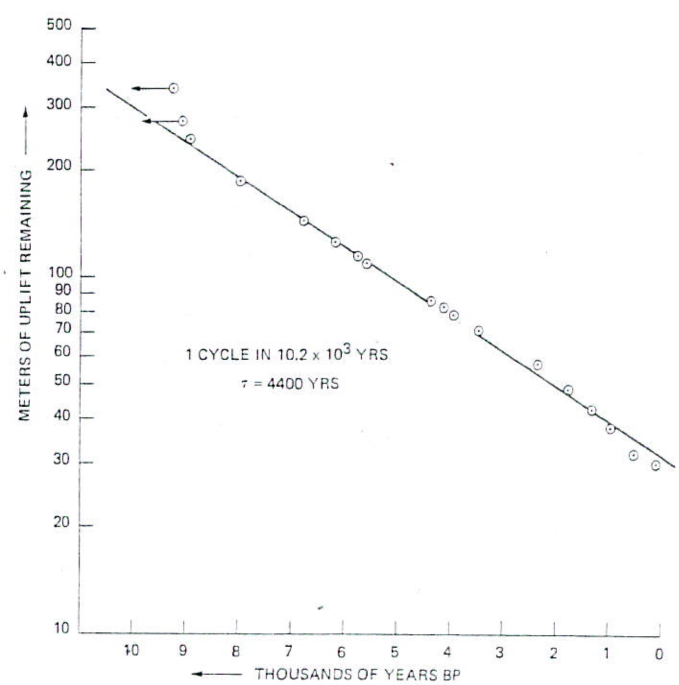

Figure IV-38. Demonstration that the uplift in central Fennoscandia can be well-characterized by an exponential function with a decay constant of 4400 years providing about 30 m of uplift are assumed to remain at present. Data are from Table IV-10. Chronology past 8000 BP may be in error due to missing varves in varve chronology (see Section IV.E.1, Figure IV-40). Arrows show suggested correction of 800 years (Stuiver, 1971).

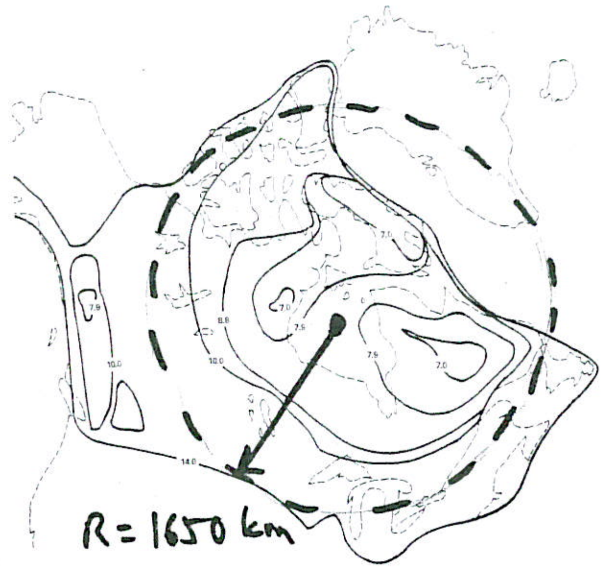

Figure IV-10. Isochron map showing the retreat of the last ice in North America sketched from a more detailed map by Prest (1969). Comparison to Figure IV-9 may suggest uncertainties in isochron determination. Isochrons are in thousands of radiocarbon years BP.

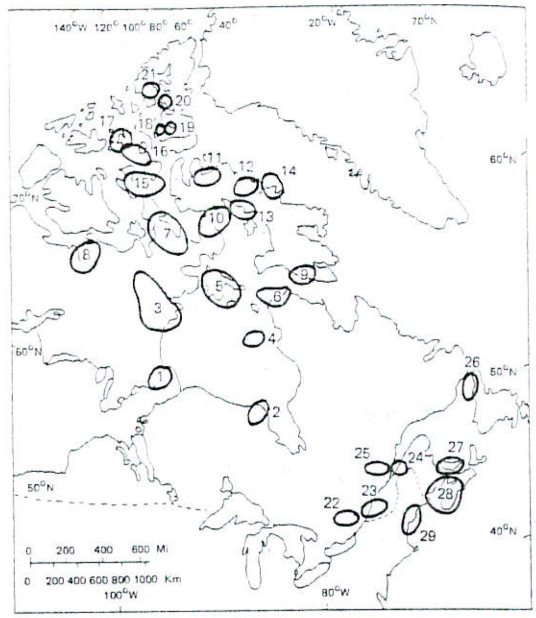

Figure App. VII-7. Areas for which emergence data have been compiled by Walcott (1972a). Data are tabulated in Table App. VII-3.

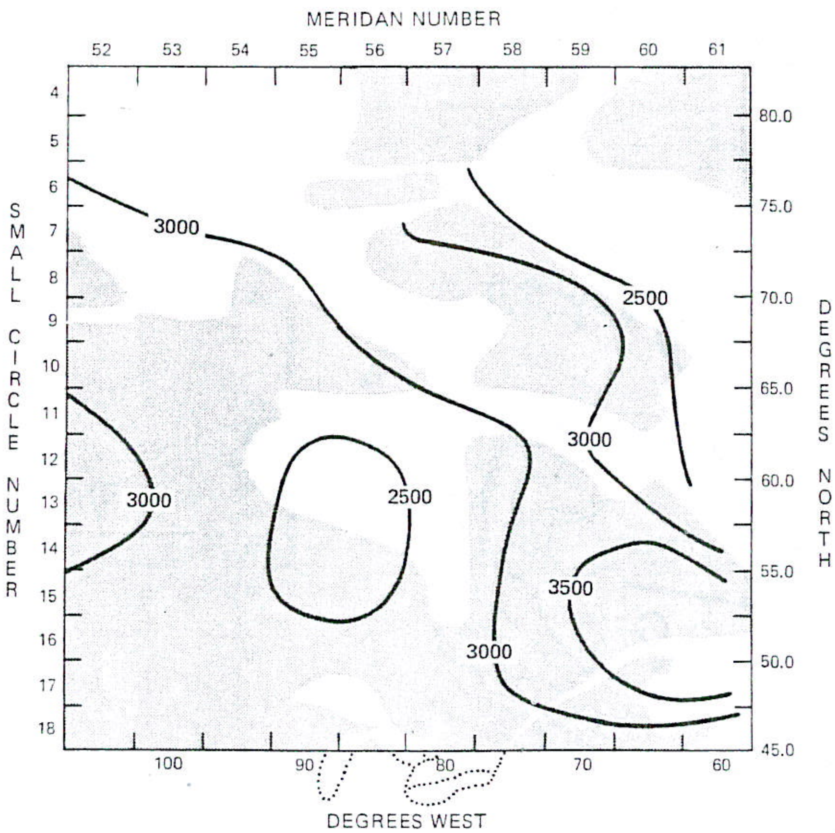

Figure IV-62. The spatial variation of decay constants characterizing the uplift of Model #1′ in Canada between 7000 and −2000 years BP (model time). The least squares fit was made to seven uplift values at each location (T = 7, 6, 5, 4, 2, 0, −2 thousand years BP).

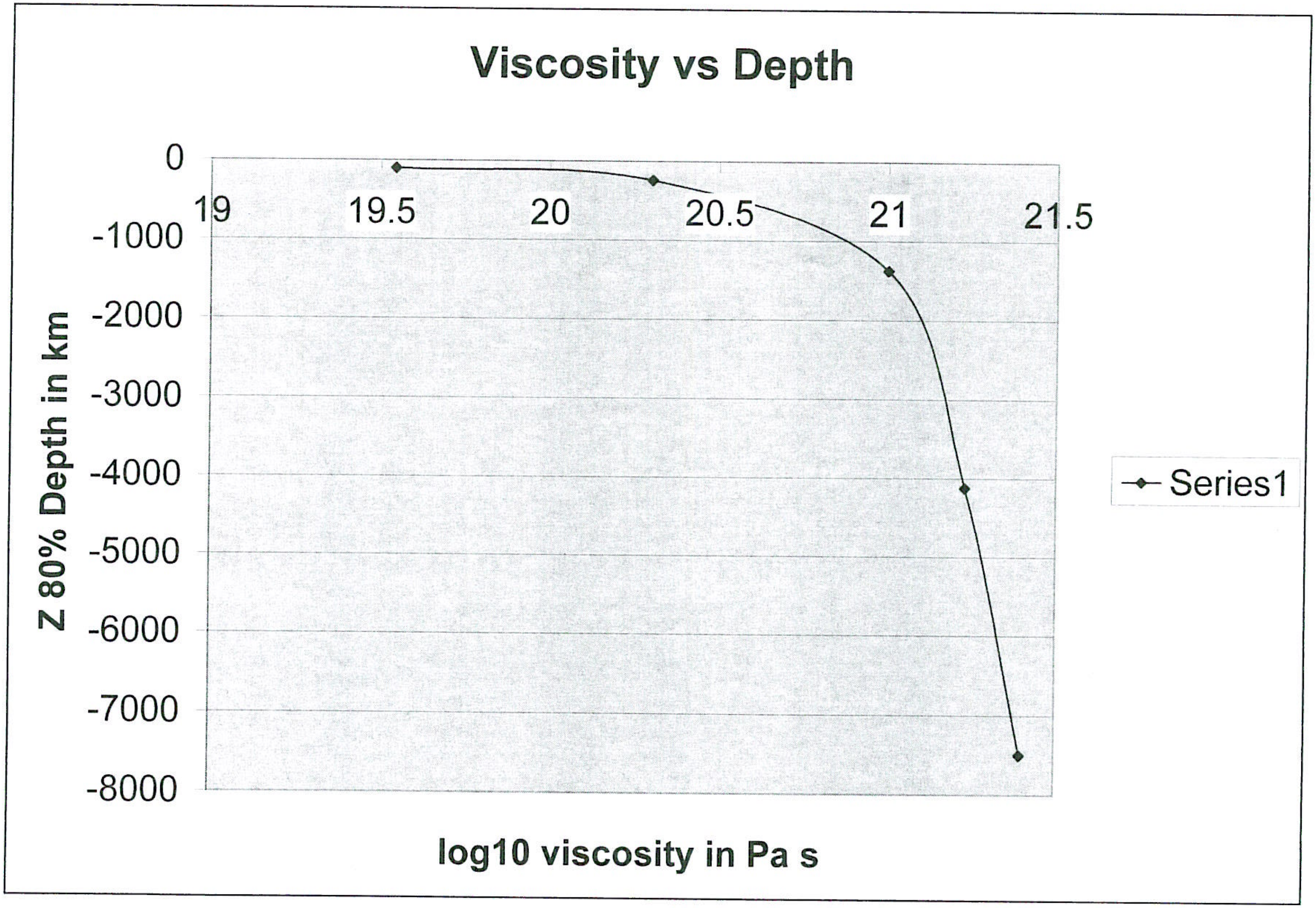
Viscosity vs Depth
0
-1000
-2000
-3000
-4000
-5000
-6000
-7000
-8000
19
19.5
20
20.5
21
21.5
Z 80% Depth in km
log10 viscosity in Pa s
Series1